Journal of Nanoparticle Research **1:** 243–251, 1999.

Gold nanoparticles: Production, reshaping, and thermal charging

Martin H. Magnusson[1], Knut Deppert[1], Jan-Olle Malm[2], Jan-Olov Bovin[2] and Lars Samuelson[1]
[1]*Solid State Physics, Lund University, Box 118, S-221 00 Lund, Sweden (E-mail: martin.magnusson@ftf.lth.se);*
[2]*Inorganic Chemistry 2, Lund University, Box 124, S-221 00 Lund, Sweden*

Received 1 December 1998; accepted in revised form 4 March 1999

Key words: gold, nanoparticles, size selection, thermal charging, particle synthesis

Abstract

Gold nanoparticles are of great interest for various nanoelectronic applications, e.g., for making single electron transistors or very fine leads to molecular size entities. For this and other applications, it is important that all particles have controllable size and shape. In this paper, we describe the production of size-selected gold aerosol particles in the 20 nm range made by evaporation in a high-temperature tube furnace and subsequent size selection. To obtain spherical particles, it was necessary to reshape the particles at high temperature, which was investigated for temperatures between 25°C and 1200°C. High-resolution transmission electron microscopy showed that the degree of crystallinity became higher for higher reshaping temperature. During reshaping at high temperature, an anomalous charging behavior was discovered, whereby negatively as well as positively charged particles became multiply negatively charged. Possible mechanisms for explaining this thermally activated phenomenon are discussed.

Introduction

In materials science and in the study of mesoscopic physics, there is a demand for nanoparticles as building blocks. In general, the nanoparticles need to be of high quality, i.e., contamination-free and preferably single crystalline. For certain applications, e.g., where size quantization effects are studied, the particles also ought to have a narrow size distribution. In this respect, aerosol technology is advantageous, since it is a gas phase, continuous and simple production method that also allows for good size selection (Deppert et al., 1998).

We have chosen to work with gold because it is an inert material and will not oxidize prior to or during further experiments. In addition, gold requires a fairly high temperature to be vaporized. Thus, the study gives indications on the feasibility of producing particles of other materials with a similar low vapor pressure in the same way.

A well established method for producing gold nanoparticles with a narrow size distribution is colloid chemistry, which is known since many years (Faraday, 1857). Problems with the wet chemical approach, as compared to gas methods, include a higher level of contaminants, risk of oxidation (though not for gold) and the non-obvious chemistry involved when a colloid of a new material is to be produced.

The oldest reference that we have found to gold nanoparticles made by physical means, also by Faraday (1857), involved electrical explosion of a gold wire in different atmospheres and collection of the particles on various substrates. A modern approach is to use low-pressure evaporation and condensation in a stream of inert gas (Granqvist & Hunderi, 1977). This method can be extended to compound particles (Patil et al., 1994). At atmospheric pressure, it is possible to use a gold mesh to get a high rate of evaporation below the melting point (Okuyama, 1998) or to use a gold-covered tungsten wire (Schleicher et al., 1993).

To date, we have not found any published result concerning production of gold aerosols using the evaporation/condensation technique with pure molten gold as source material where the resulting particles were classified according to their size.

In the sections following the Experimental, we first describe how the production and thermal charging of gold particles is dependent on the temperature in the evaporation oven. Second, we present a study of the reshaping process, supported by transmission electron microscopy (TEM) and third, we report on an anomalous, thermally activated, recharging effect.

Experimental

A schematic of the aerosol fabrication apparatus is shown in Figure 1. Furnace 1 is capable of reaching 2000°C and its inner tube is made of pyrolytic graphite. A ceramic boat (high purity pyrolytic boron nitride) containing the material to be aerosolized is placed inside the tube furnace, which is heated to achieve a high enough vapor pressure of the material. A flow of nitrogen carrier gas (purity >99.998%) is passed through the furnace at 1.68 l/min and the material vapor condenses into an aerosol (Scheibel & Porstendörfer, 1983).

The particles are size selected in a so-called differential mobility analyzer (DMA), which classifies charged particles according to their mobility in an electric field (Knutson & Whitby, 1975). This mobility is roughly inversely proportional to the particle diameter. Our home-built DMA, of the Vienna type (Winklmayer et al., 1991), is run with a sheath gas flow of 10 l/min. The ratio between the carrier and sheath gas flows is 17%, which is also the theoretical full width at half maximum of the aerosol size distribution after the DMA. Since a TEM calibration of the absolute diameters has not been done, all DMA diameter values must be interpreted cautiously. A limited study shows that the diameter given by the DMA is too large. The overestimate for 8 nm particles may be up to 50% (Deppert et al., 1996a), but the error is smaller for larger particles.

In our setup, size selection can only be done for charged particles. The aerosol is charged by passing it through a photoelectric charging device using UV-light (222 nm) to create free electrons and positively charged particles (Burtscher et al., 1982). The free electrons can then charge the neutral particles, and the net effect is an aerosol consisting of uncharged and both positively and negatively charged particles. Due to the Coulomb blockade effect in such small objects, multiply charged particles are rare. Thus, the charging efficiency is lower the smaller the particles are. For particles less than 20 nm in diameter, about 99% of them are uncharged, which limits the yield.

When the newly formed aerosol leaves the production furnace, it consists of agglomerates of small primary particles, around 3–5 nm in diameter. In order to make the particles compact, they are reshaped in a second furnace. To monitor the change in the particle diameter, a second DMA, of the same kind as the first one, is used. By setting the first DMA to a fixed diameter and scanning the second, we can obtain the size distribution of the particles after the reshaping furnace, for different temperatures. The particle concentration is measured with a home-built

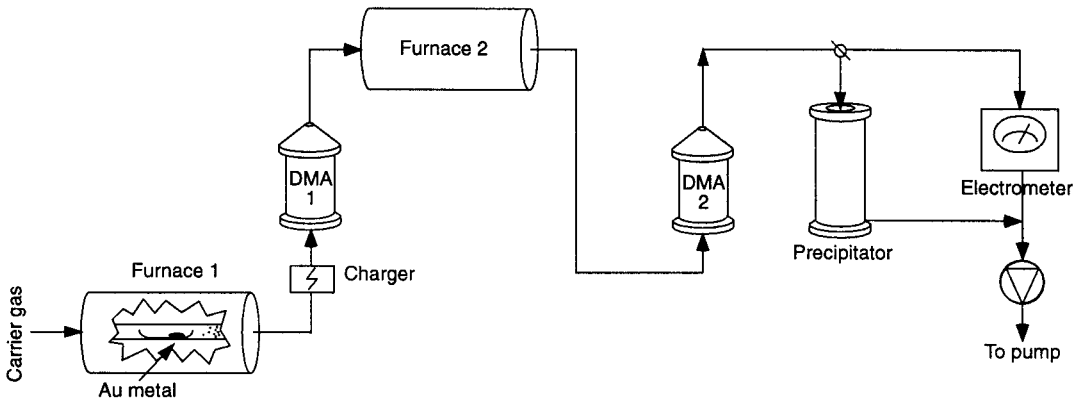

Figure 1. Schematic of the nanoparticle fabrication apparatus.

electrometer, where it is assumed that the particles are singly charged.

In the present study, high purity gold (99.9999%) was aerosolized at temperatures up to 1700°C and the reshaping process was studied from ambient temperature up to 1200°C, which is well above the bulk melting temperature of gold (1065°C). To obtain morphological information, high-resolution TEM was used. The particles were collected on standard grids for TEM in an electrostatic precipitator (Deppert et al., 1996b), and analyzed *ex situ*. We studied the reshaping of both negatively and positively charged particles by changing the polarities in the two DMAs. We also sometimes used opposite polarities in the two DMAs in order to investigate an anomalous recharging effect, which we describe below. The particles were most often negatively charged and if they were positively charged, this is explicitly stated.

Particle production

As the temperature of the production furnace is raised, it is well known that both the mean particle diameter and the number concentration increase at the expense of the production of the smallest particles and that the size distribution usually is lognormal (Scheibel & Porstendörfer, 1983). Our measurements, shown in Figure 2, confirmed this behavior: 5 nm particles became detectable at 1400°C and a high concentration, with a maximum at 30 nm, was reached at 1650°C. Since we were interested in particle production and not in measurement of the true size distribution, we did not normalize our data with the width of the size distribution of the DMA. We also would like to point out that our electrometer could not measure particle concentrations below 10^3 cm^{-3}, so there was probably a minor particle production even below 1400°C.

When the photoelectric charger was turned off, the signal in the electrometer did not disappear completely, but decreased by a factor of about 10, cf. Figure 3. Since only charged particles can be classified and measured, we conclude that thermionic emission occurs in the gold vapor or in the newly formed aerosol. Both negatively and positively charged particles could be detected, and the concentration of negative particles was slightly higher than that of positive ones.

With thermal charging only, particles were not detectable below 1500°C. The maximum of the size distribution of the thermally charged particles appeared at a somewhat smaller size than for the intentionally charged ones, at equal evaporation temperatures.

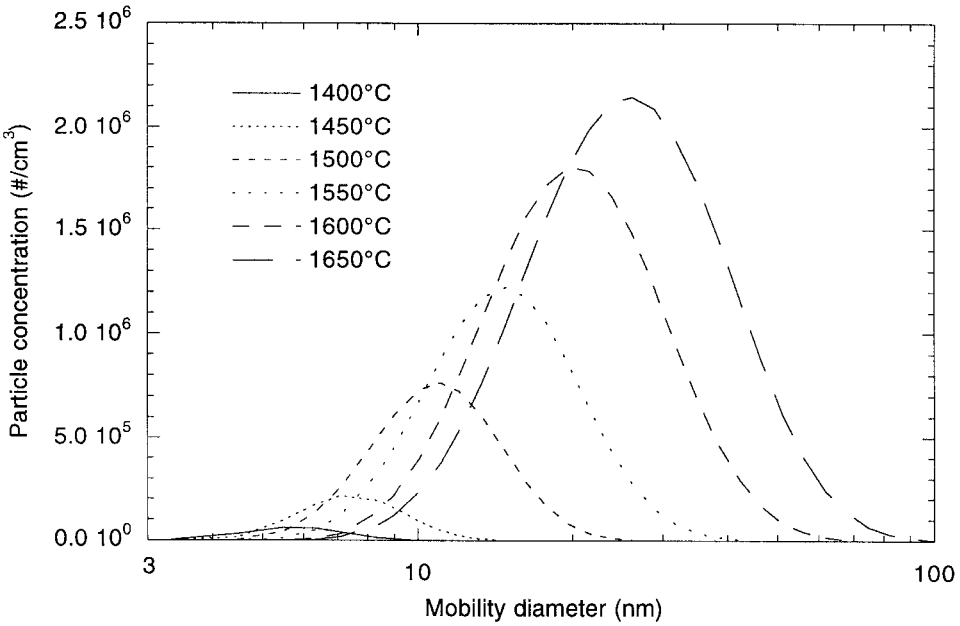

Figure 2. Mobility scans of gold particles produced at different temperatures of the evaporation furnace, measured with only the first DMA (i.e., without reshaping) and with photoelectric charging turned on. The particles were negatively charged.

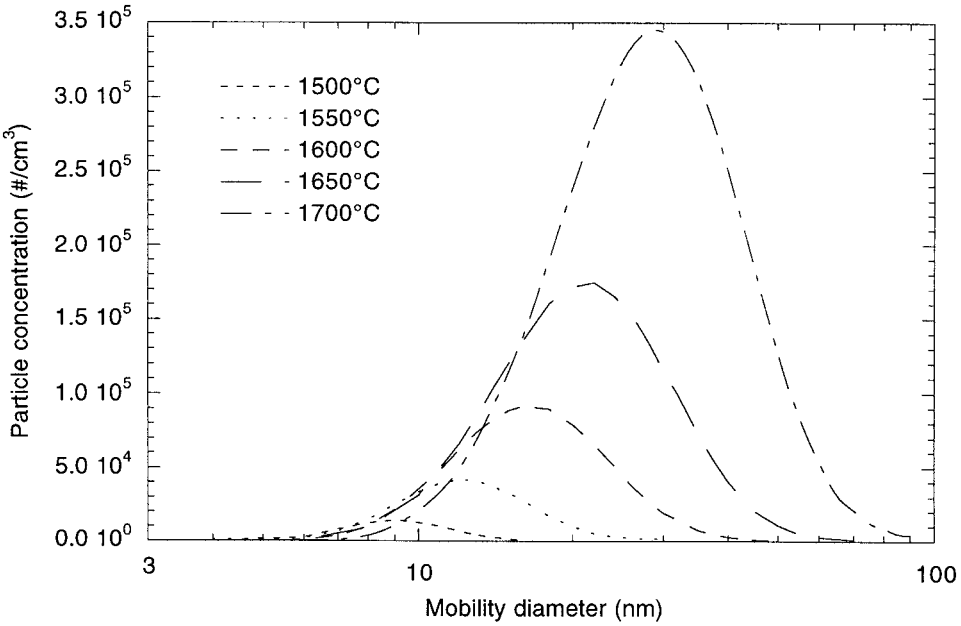

Figure 3. The same measurement as in Figure 2, but with photoelectric charging turned off. The particles were negatively charged.

We attribute this to the higher efficiency of photoelectric charging for larger particles, which shifts the distribution for the intentionally charged particles to larger sizes.

Reshaping

In this paper, we have chosen the terms 'reshaping' and 'compact' to describe the treatment of the particles and their resulting shape, respectively. We avoid the more common term 'sintered' since we expose the particles to temperatures both below and above the melting temperature, and therefore the term sintering might be misleading. Since particles that have been molten often become faceted, claiming them to be spherical would in those cases be false.

When a material with a melting point much above ambient temperature is aerosolized by evaporation and condensation, the particles will often be agglomerates of smaller particles (cf. Figure 4a). This can be avoided either by preventing agglomeration by diluting the aerosol or having the particles grow in a vacuum, or by reshaping the particles after the agglomerates have formed. When reshaped in a sufficiently hot furnace, the particles become compact (cf. Figure 4b,c) and their mean mobility diameter decreases compared to the original value, since the air resistance is smaller for a spherical particle of the same mass (Hinds, 1982). Actual melting of the particles is not necessary for the particles to become compact and spherical (Schmidt-Ott, 1987; Seto et al., 1995); solid state diffusion is often sufficient.

Figure 5 shows how the mean particle diameter of gold particles changed with the temperature in the reshaping furnace. The data points represent the maxima of the size distributions for particles reshaped at the respective temperatures; this is a simple and good measure of the mean particle diameter if the size distribution is narrow. The stability of the particle diameters in the range 300–1100°C is apparent. What is not shown is that the particle concentration dropped steadily, which we attribute to losses to the furnace walls due to thermophoresis. The slight difference between the size given by the first and the second DMA for untreated particles can be explained by the fact that no two DMAs are identical. Another explanation could be coagulation during the passage through the machine. However, coagulation should be limited since, after sorting, all particles are unipolarly charged and their number concentration is much reduced. The lack of data for the 60 nm particles at high temperature is due to the anomalous recharging described in the next section.

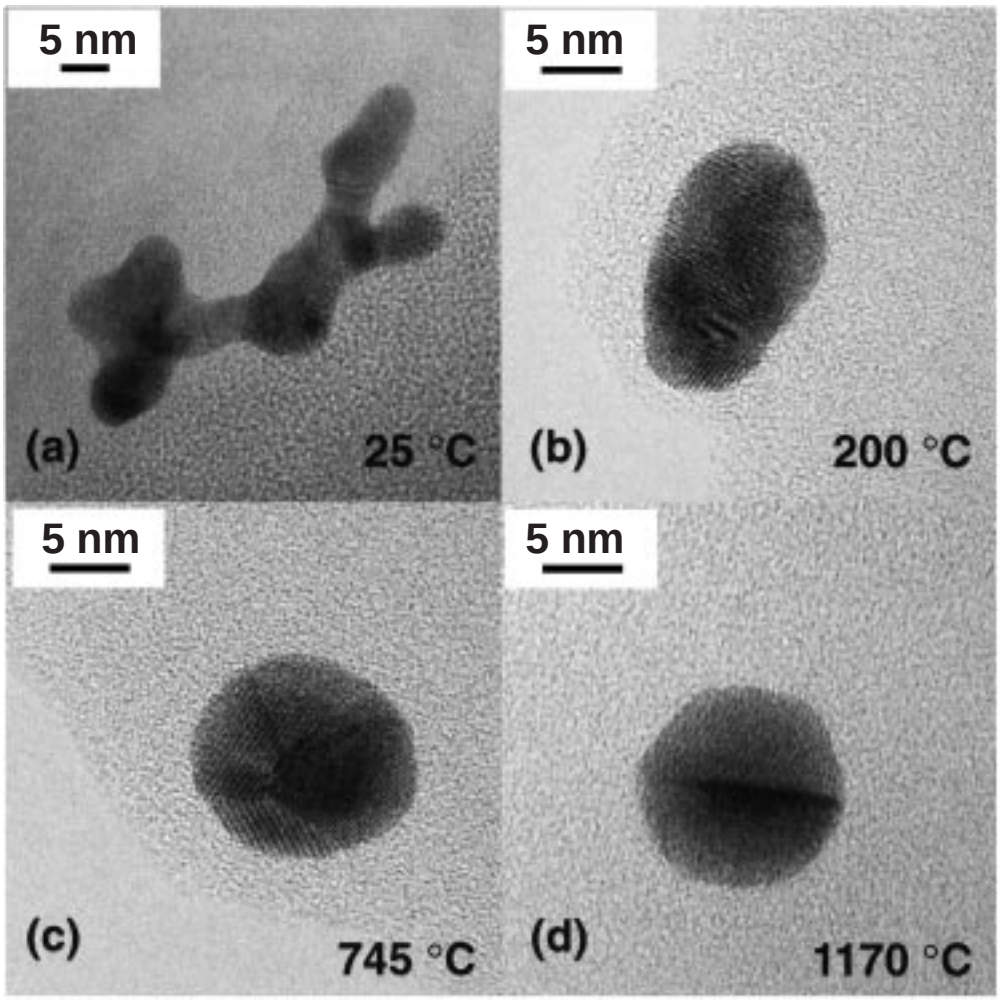

Figure 4. TEM images of gold particles reshaped at different temperatures. Note how the compacting of the particles is accompanied by an increase in crystallinity. Also, note the apparent faceting of the particle in (d) reshaped at 1170°C. The diameter setting in the first DMA was 30 nm for (a), and 18 nm for (b–d), whereas the second DMA was set for maximum yield.

Above a certain temperature, the diameter did not change, which is taken as evidence that the particles had reached full density and become almost spherical. However, the degree of particle crystallinity is not given by a DMA measurement, so a TEM investigation of the particle morphology was needed for a better understanding of the reshaping process.

The fact that the mean particle size did not change for temperatures above 300°C does not mean that the reshaping was complete. Untreated particles (Figure 4a) have an irregular shape, but already at 200°C they have become compact and nearly spherical (Figure 4b). The compact particles are still polycrystalline, even at 745°C (Figure 4c), while particles that have been molten at 1170°C are almost single crystalline (Figure 4d), although they may still contain defects.

The particle in Figure 4d is faceted, and although it contains a defect, some crystalline order seems to extend over the entire particle, since the facets are symmetrical. It should be pointed out that this particle is typical for particles that have been molten during reshaping. Many of them have facets and a single defect running through the center. An earlier investigation on sintering of gold particles, albeit larger and in a silica matrix, showed particles that were similar

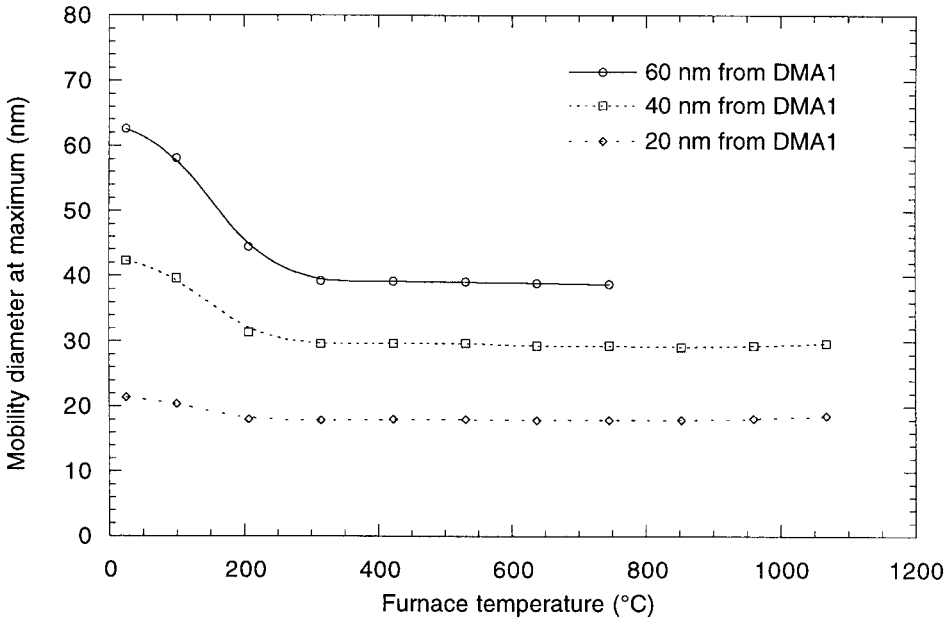

Figure 5. The resulting mean particle diameter after reshaping gold particles at different temperatures, as measured with the second DMA. The points are measurements and the lines are only guides for the eye. The first DMA was set to produce 20, 40, and 60 nm particles, respectively.

to ours (McGinn et al., 1982). For most applications, e.g., for single electron devices, our nanoparticles can be regarded as ideal.

Recharging effect – observations

As the reshaping temperature was raised above 600°C, an unexpected phenomenon occurred, which, to our knowledge, has not been reported previously. At the higher reshaping temperatures, new peaks appeared in the size distribution, cf. Figure 6a. The positions of the peaks correspond exactly to where spherical particles of one diameter would be found, if they were charged singly, doubly, triply, etc. The electrical mobility is directly proportional to the charge on the particle. Thus, multiply charged particles appear smaller when classified with a DMA.

After measuring the mobility distribution of the gold particles after having been reshaped at 1068°C, cf. Figure 7, we bypassed the second DMA, and collected all particles on a standard grid for TEM. A TEM measurement of the diameters of 139 individual particles was performed, and this showed that they all fell within the same size class. A histogram of the particle diameters is presented in the inset of Figure 7, showing that the true particle size distribution was narrow, with a standard deviation of 9% of the median diameter. In addition, the aforementioned discrepancy between the DMA and TEM sizes is evident.

To further investigate the phenomenon, we changed the polarity of the two DMAs, to select and measure positively charged particles instead. The result, shown in Figure 6b, was that the behavior was identical to the case of negatively charged particles below 500°C. As the temperature in the reshaping furnace was raised further, the particles seemed to disappear, even though the vapor pressure of gold was never high enough for the particles to evaporate. In contrast, the negatively charged particles remained until 1200°C. We then reversed the polarity of the second DMA once more, so that negatively charged particles were detected, while the first DMA selected positive ones. We found that the particles had changed their polarity from positive to negative and that they had even become doubly and triply charged (cf. Figure 6c).

It should be noted that the curves plotted in Figure 6 are based on the signal from the electrometer. If the particles are multiply charged, the actual particle concentration should be divided by the multiplicity. This might be verified by a measurement with a ultrafine condensation particle counter (UCPC). However, we

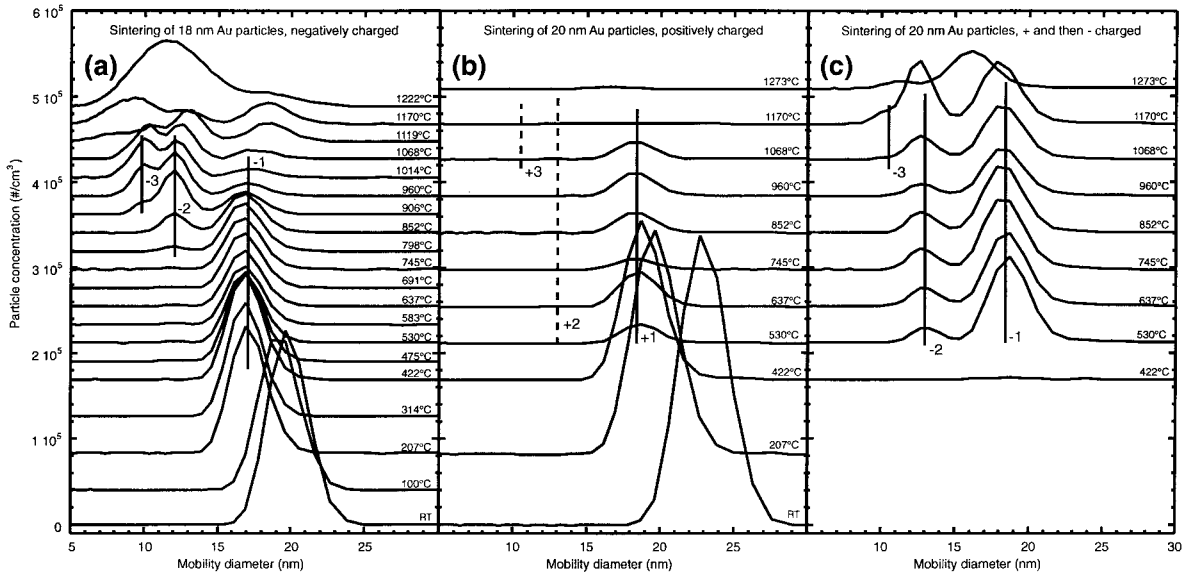

Figure 6. Mobility scans of 20 nm gold particles displaced according to the reshaping temperature. In (a) both DMAs were set to sort negative particles and in (b) both were set for positive particles. In (c) the first DMA selected positive particles while the second classified negative ones. In all figures, the lines labeled ± 1, ± 2, ± 3 mark the positions where peaks corresponding to singly, doubly, and triply charged particles should appear if all particles had the diameter marked by the line at ± 1. Note that peak heights at $\pm n$ charges should be divided by n in order to obtain the true particle concentration, since the measurement was made with an electrometer.

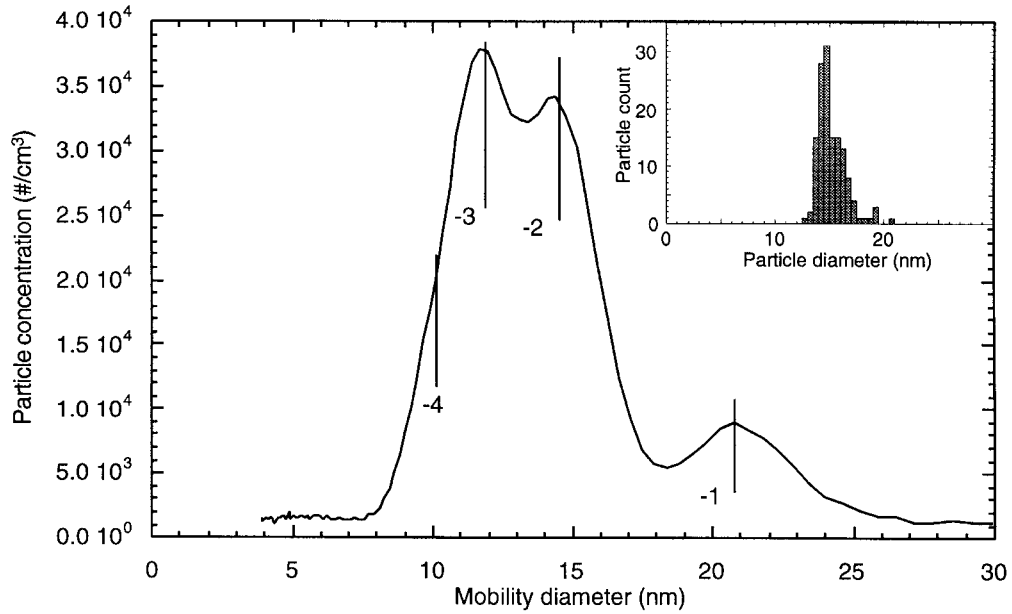

Figure 7. Mobility scan for gold particles reshaped at 1068°C, with multiple charge peaks marked as in Figure 6. After this measurement, the second DMA was bypassed and all particles were collected on a TEM grid. The size distribution of the particles as measured by TEM is shown in the inset, which clearly shows that the particles are monodisperse, albeit with the usual discrepancy between the sizes measured by DMA and TEM.

cannot use one, since the UCPC is incompatible with our high-purity system, and since it cannot measure high particle concentrations without dilution.

To test whether the phenomenon occurs only for gold, we performed a limited study for tungsten particles. This gave the preliminary result that recharging occurs, with no significant differences as compared to gold. Further investigation is necessary before any certain conclusions can be drawn.

Recharging effect – discussion

Since we observe a temperature dependent recharging of the particles, and one that goes toward the negative, we must have a source of electrons in or near the hot zone of the reshaping furnace. We have further considered the possibility that the particles lose positive gold ions, but we have no suggestion as to how this might happen. The obvious candidates for the electron source are the particles themselves, the carrier gas or the furnace wall. The temperature dependence of the relative peak heights, shown in Figure 8, could be interpreted as an activation energy of 2–3 eV. This is too small to be explained by recharging of the particles by each other; the work function of gold is 5.4 eV, (CRC, 1997). More importantly, it is ruled out by the fact that the positive gold particles did not become multiply charged, but became negative instead.

The carrier gas, nitrogen, with an ionization energy of 15.6 eV (CRC, 1997), should not ionize in this temperature range, and therefore, it can hardly transfer charge to or from the particles. The same holds for the trace amounts of contaminants in the carrier gas. Reactions between these contaminants might release charge, but we see no reason why this only should charge particles negatively.

The last candidate for the source of electrons is the furnace wall which, according to the manufacturer, is 99.7% alumina. Energy dispersive X-ray spectroscopy (EDX) of the material in the wall of the reshaping furnace found only aluminum. To test whether the alumina tube was the source of electrons, we inserted a grounded tantalum foil into the reshaping furnace, covering the interior surface for more than the length of the hot zone. Tantalum has a work function of 4.25 eV (CRC, 1997). This did not eliminate the thermal charging, but instead made the process slightly more efficient. This leaves us without an obvious candidate for the electron source.

It is worth noting that the great majority of the gold particles receive this extra charge since the total particle concentration does not drop more than could be expected from thermophoresis. This means that we have a very efficient unipolar charger. Considering the

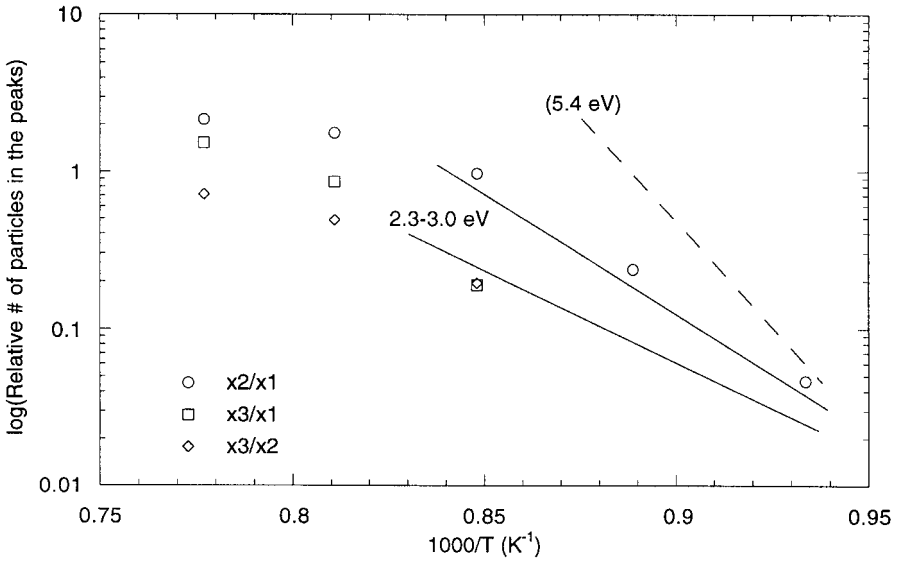

Figure 8. The peak heights in Figure 6a, relative to the singly (◯, □) and to the doubly (◇) charged peaks, plotted in an Arrhenius-like plot. The peak heights were corrected for multiple charges. The apparent activation energy for the thermal recharging is 2.3–3 eV. The dashed line, corresponding to the work function of gold, is included for comparison.

low yield obtained with conventional chargers for such small particles, this would be a great improvement if it were to work for higher particle concentrations. We are currently investigating the feasibility of using this setup as a new type of charging device for gold particles.

Summary

We have produced size-selected gold particles in the 20-nm size range by aerosol means. After production, the particles had an irregular shape, but after having been reshaped at high temperature, they became nearly spherical and nearly single crystalline. Particles reshaped at temperatures above the melting point often became faceted. Reshaping at high temperature led to thermally activated recharging of the particles, whereby all particles became multiply negatively charged, regardless of their initial charge state. Nothing conclusive can be said about the mechanism behind the phenomenon without further investigation.

Acknowledgements

This work was performed within the Nanometer Structure Consortium and was financed by NFR, TFR, NUTEK, SSF and the ESPRIT CHARGE program, project No. 22953.

References

Burtscher H., L. Scherrer, H.C. Siegmann, A. Schmidt-Ott & B. Federer, 1982. Probing aerosols by photoelectric charging. J. Appl. Phys. 53, 3787–3791.

CRC, 1997. CRC Handbook of Chemistry and Physics. CRC Press, Boca Raton.

Deppert K., J.-O. Bovin, J.-O. Malm & L. Samuelson, 1996a. A new method to fabricate size-selected compound semiconductor nanocrystals: Aerotaxy. J. Cryst. Growth 169, 13–19.

Deppert K., F. Schmidt, T. Krinke, J. Dixkens & H. Fissan, 1996b. Electrostatic precipitator for homogeneous deposition of ultrafine particles to create quantum-dot structures. J. Aerosol Sci. 27, S151–S152.

Deppert K., M.H. Magnusson, L. Samuelson, J.-O. Malm, C. Svensson & J.-O. Bovin, 1998. Size-selected nanocrystals of III–V semiconductor materials by the aerotaxy method. J. Aerosol Sci. 29, 737–748.

Faraday M., 1857. Experimental relations of gold (and other metals) to light. Philos. Trans. R. Soc. 147, 145–181.

Granqvist C.G. & O. Hunderi, 1977. Optical properties of ultrafine gold particles. Phys. Rev. B 16, 3513–3534.

Hinds W.C., 1982. Aerosol Technology: Properties, Behavior, and Measurement of Airborne Particles. J. Wiley, New York. p. 48.

Knutson E.O. & K.T. Whitby, 1975. Aerosol classification by electric mobility: Apparatus, theory, and applications. J. Aerosol Sci. 6, 443–451.

McGinn J.T., A. Greenhut, T. Tsakalakos & J. Blanc, 1982. Formation of fault structures during coalescence and growth of gold particles in a fused silica matrix. I. Acta Metall. 30, 2093–2102.

Okuyama K., 1998. Personal communication.

Patil A.N., R.P. Andres & N. Otsuka, 1994. Synthesis and minimum energy structure of novel metal/silica clusters. J. Phys. Chem. 98, 9247–9251.

Scheibel H.G. & J. Porstendörfer, 1983. Generation of monodisperse Ag- and NaCl-aerosols with particle diameters between 2 and 300 nm. J. Aerosol Sci. 14, 113–126.

Schleicher B., H. Burtscher & H.C. Siegmann, 1993. Photoelectric quantum yield of nanometer metal particles. Appl. Phys. Lett. 63, 1191–1193.

Schmidt-Ott A., 1987. New approaches to *in situ* characterization of ultrafine agglomerates. J. Aerosol Sci. 19, 553–563.

Seto T., M. Shimada & K. Okuyama, 1995. Evaluation of sintering of nanometer-sized titania using aerosol method. Aerosol Sci. Technol. 23, 183–200.

Winklmayer W., G.P. Reischl, A.O. Lindner & A. Berner, 1991. A new electromobility spectrometer for the measurement of aerosol size distribution in the range from 1 to 1000 nm. J. Aerosol Sci. 22, 289–296.